ノート

# $\alpha$-Al$_2$O$_3$ 担持 Pt ナノ粒子触媒の CO 酸化活性と着火現象

田口 明*，尾崎 智弘

富山大学　研究推進機構　水素同位体科学研究センター

〒930-8555　富山市五福 3190

## Ignition-extinction phenomena in CO oxidation reaction over "dry" impregnated platinum nanoparticles on α-Al$_2$O$_3$

Akira Taguchi*, Tomohiro Ozaki

Hydrogen Isotope Research Center

Organization for Promotion of Research, University of Toyama

Gofuku 3190, Toyama 930-8555

**Abstract**

Catalytic CO oxidation activity of α-Al$_2$O$_3$ supported Pt, prepared by the sputter deposition method was investigated. The oxidation activity showed the structure sensitivity with negative particle effects. An ignition-extinction phenomenon was observed in CO oxidation reactions arising from the "mass-transfer limitation" owing to the high turn-over frequency.

**Research note**

Recent advances in the synthesis and characterization of nanosized particles have promoted an extensive search for methods to prepare highly efficient nanostructured catalysts [1-3]. Sputter deposition, a "dry" impregnation method that does not use any solvent or liquid for catalyst preparation, has gained attention because it has several advantages as compared to the conventional "wet" impregnation method [4-6].   We have investigated the preparation and growth of Pt nanoparticles on $Al_2O_3$ by FE-SEM and CO chemisorption study [7].   Pt nanoparticles formed in the early stages of sputter deposition were well isolated, and the particle size distribution of Pt nanoparticles was narrow.   Longer sputter deposition resulted in growth and coalescence of Pt nanoparticles.

In this note, the catalytic activity of these obtained $Pt/Al_2O_3$ was studied from the oxidation of CO to $CO_2$.   An intrinsic ignition-extinction phenomena has been observed.

The $\alpha$-$Al_2O_3$ supported Pt ($Pt/Al_2O_3$) used in this study was prepared by a barrel-sputtering system as described in our previous paper [7].   The RF power and Ar gas pressure were 25 W and 0.8 Pa, respectively.   Depending on the duration of the sputter deposition, the deposition amount and the diameter of Pt particle obtained were changed.   The number of Pt atom on surface, corresponding to the amount of CO adsorbed, and the Pt dispersion calculated from CO chemisorption study were listed in Table 1.   Here, the catalysts are denoted as Pt($x$), where $x$ represents the Pt dispersion determined by CO chemisorption study [7].

The CO oxidation reaction was studied in a fixed-bed flow reactor (6 mm inner diameter) under atmospheric pressure.   Two thermocouples were used, one located in the catalyst in the fixed bed to measure the temperature, and the other on the outside of the quartz reactor to control the reaction temperature via a heater.   Reactor effluent gas was analyzed with an on-

Table 1 Preparation, Pt particle diameter and Pt dispersion of Pt/Al$_2$O$_3$ [7].

| Sample ID | Sputter-deposition time (min) | Pt deposition amount (wt%) | Pt diameter (FE-SEM) (nm) | Pt surface (/g) | Pt dispersion* (-) |
|---|---|---|---|---|---|
| Pt(0.70) | 4 | 0.021 | 1.8 | 2.18×10$^{18}$ | 0.70 |
| Pt(0.50) | 5 | 0.032 | 2.7 | 1.57×10$^{18}$ | 0.50 |
| Pt(0.31) | 7 | 0.056 | 3.9 | 0.95×10$^{18}$ | 0.31 |
| Pt(0.25) | 9 | 0.075 | 4.5 | 0.77×10$^{18}$ | 0.25 |
| Pt(0.18) | 20 | 0.136 | 5.1 | 0.57×10$^{18}$ | 0.18 |

* Pt dispersion was investigated at 0 ºC after thermal treatment at 250 ºC under H$_2$/He flow.

lined gas chromatograph (Shimadzu; GC-8A, column; MS-5A) equipped with TCD.    For the reaction test, a mixture of Pt/Al$_2$O$_3$ (0.10 g) and unsupported α-Al$_2$O$_3$ (2.90 g) as the dilutant was loaded into the reactor.    The catalyst was heated to 250 ºC at a ramp rate of 5 ºC/min under He flow.    At this temperature, fluid gas was changed to a mixture of H$_2$ (50 %) and He balance, and this temperature was maintained for additional 1 h.    After cooling to room temperature under He flow, the fluid gas was switched to the mixture of CO (0.5%), O$_2$ (5.0%) and He balance with a total flow rate of 120 ml/min to start the reaction.    After 30 min, the effluent gas was analyzed by gas chromatography.    The temperature was raised from room temperature to an appropriate one at a ramp rate of 5 ºC/min, and then the effluent gas was analyzed after 30 min.    Subsequently, the temperature was raised and catalytic activity was measured in the same manner.    This sequence was repeated up to the appropriate temperature where the CO conversion reached 100 %.    After reaching 100 % conversion, the temperature was lowered at decrements of 5 ºC until the conversion decreased to a certain value.    The CO conversion was calculated from the following equation:

$$\text{Conv.} = \frac{\left([CO]_{in} - [CO]_{out}\right)}{[CO]_{in}} \times 100$$

Here, $[CO]_{in}$ and $[CO]_{out}$ are the concentration of CO in the inflow and the effluent gas,

respectively.

Figure 1 shows the oxidation of CO to $CO_2$ over Pt(0.70) and Pt(0.25) as a function of temperature.　The CO oxidation activity of Pt catalysts was typically low as compared to other transition metals and precious metals [8-10].　Thus, for instance, about 5 % conversion was observed at 165, 170, 180, 190 and 200 ºC for Pt(0.18), Pt(0.25), Pt(0.31), Pt(0.50) and Pt(0.70), respectively.　The CO oxidation conversion increased exponentially up to about 60 % with an increase in the reaction temperature, and then the conversion suddenly increased to 100 % with a further increase of 5 ºC in the reaction temperature.　This sudden increase of conversion was not due to the lack of the reactant, but rather due to the ignition phenomenon.

The conditions where the conversion reached 100% (Conv.100) can be predicted using the following relationship:

$$[CO]_{feed} = TOF \times Pt_{surface}$$

Here, $[CO]_{feed}$ represents the number of CO molecules fed in a unit of time ($2.6875 \times 10^{17}$ number/sec).　Thus, the expected temperature where the conversion reached 100 % can be calculated from the Arrhenius equation as follows:

$$T = -\left(\frac{E_a}{R}\right) \cdot \left(\frac{1}{\ln(TOF) - \ln(A)}\right)$$

$$= -\left(\frac{E_a}{R}\right) \cdot \left(\frac{1}{\ln\left(\frac{[CO]_{feed}}{Pt_{surface}}\right) - \ln(A)}\right)$$
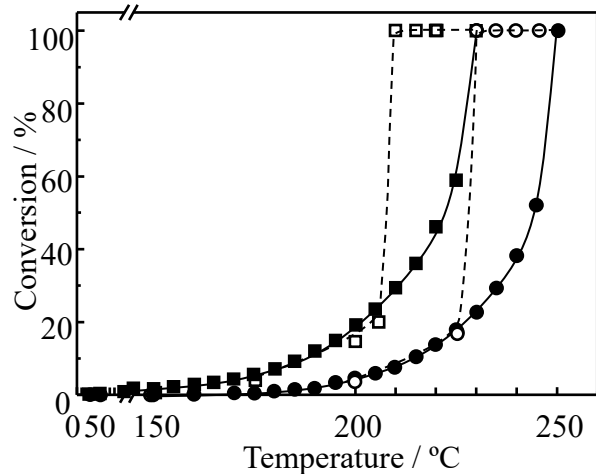
The temperatures of Conv.100 for Pt(0.18),



Fig. 1　The conversion of CO to $CO_2$ as a function of reaction temperature over $Pt/Al_2O_3$ prepared. (●) Pt(0.70) at rising temperature, (○) Pt(0.70) at lowering temperature, (■) Pt(0.25) at rising temperature, (□) Pt(0.25) at lowering temperature.

Pt(0.25), Pt(0.31), Pt(0.50) and Pt(0.70) were 233.3, 240.5, 242.5, 251.0 and 257.9 ºC, respectively.   These values were about 5–10 ºC higher than the empirical ones shown in Figure 1.   This fact supports the idea that the sudden increase of conversion was not due to the lack of the reactant, but to the ignition phenomenon.

It should be noted that the catalysis experiments with different amounts of catalyst, i.e., Pt/Al$_2$O$_3$ (0.06 g) and CO (0.5 %), O$_2$ (5%) and He balance with a total flow rate of 80 ml/min, gave almost the same reaction curves as in Figure 1.   Thus, it turn out that such an ignition phenomenon arises from the hot spot in the exothermic reaction ( $CO + \frac{1}{2}O_2 \rightarrow$ $CO_2$, $\Delta H$ = -283.0 kJ/mol).   According to the detailed study by Bourane and Bianchi [11-13], the dominant species on a Pt surface change before and after ignition temperature.   In that study, although adsorbed CO species were dominant on Pt surface (Pt-CO) before the ignition temperature, strongly adsorbed oxygen species were covered on Pt surface (Pt-O) above the ignition temperature.   This was interpreted from the "mass-transfer limitation" owing to the high TOF [12,13].

Lowering the reaction temperature in steps of 5 ºC from the one where 100 % conversion was achieved resulted in the hysteresis in the reaction curve in Figure 1. In Pt(0.70), for example, 100 % conversion was maintained from 250.3 to 230.0 ºC, then suddenly decreased to 17.4 % at 225.3 ºC. A similar hysteresis was observed in other Pt/Al$_2$O$_3$ catalysts.   The width of hysteresis, defined as the temperature range in which the CO conversion maintained at
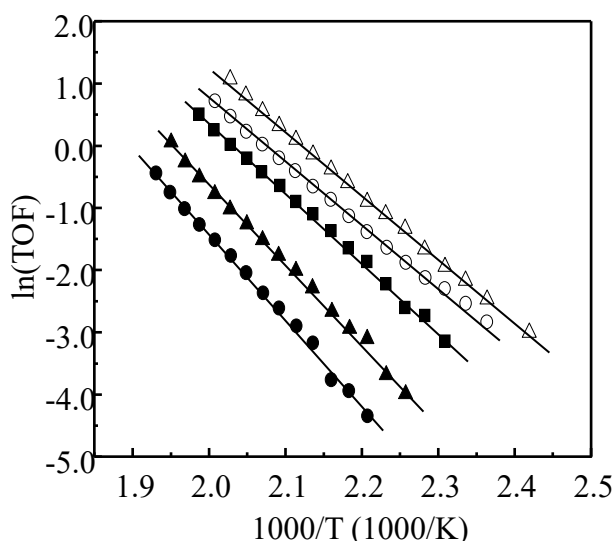


**Fig. 2**   Arrhenius plot obtained from the oxidation from CO to CO$_2$ over Pt/Al$_2$O$_3$. (●) Pt(0.70), (▲) Pt(0.50), (■) Pt(0.31), (○) Pt(0.25), (Δ) Pt(0.18).

100 %, was about 20–25 ºC and was independent of Pt/Al$_2$O$_3$.

The Arrhenius plot obtained from TOF, defined as the number of CO$_2$ molecules

**Table** 2 The Arrhenius parameter at CO oxidation over Pt/Al$_2$O$_3$

| Sample ID | Activation energy ($E_a$ kJ/mol) | Frequency factor (-) |
|---|---|---|
| Pt(0.70) | 114.93 | $2.4857 \times 10^{11}$ |
| Pt(0.50) | 105.53 | $5.6359 \times 10^{10}$ |
| Pt(0.31) | 92.63 | $6.6465 \times 10^{9}$ |
| Pt(0.25) | 82.44 | $8.4260 \times 10^{8}$ |
| Pt(0.18) | 86.03 | $3.5210 \times 10^{9}$ |

formed over each surface Pt atom per second, is shown in Figure 2. The values of $E_a$ and the frequency factor A are listed in Table 2. The $E_a$ was found to decrease with a decrease of Pt dispersion, consistent with previous papers [14,15]. The frequency factor was in the range of $10^{11}$–$10^8$ s$^{-1}$, which was in good agreement with previous papers [15-18]. It is clear from Figure 2 that the activity of CO to CO$_2$ reaction was in the order of Pt(0.18) > Pt(0.25) > Pt(0.31) > Pt(0.50) > Pt(0.70) in the entire temperature region studied. This order indicates a particle size dependence of activity, and this can be clearly seen in Figure 3.

In Figure 3, TOF at 180, 200, and 220 ºC is plotted against the Pt dispersion. Exponential decrease of the activity depending on the Pt dispersion, i.e., the particle diameter of Pt, has been clearly observed [15,19-21], indicating a structure sensitive reaction with negative particle effects according to the classification by Che and Bennett [19]. In addition, Figure 3 reveals that there were two different activities, which became clear when the reaction temperature was raised. They were in low Pt dispersion, corresponding to Pt(0.18), Pt(0.25) and Pt(0.31), and in high Pt dispersion of Pt(0.50) and Pt(0.70). Generating this grouping might give an indication of the effect of agglomeration of Pt nanoparticles. The dispersion dependency in Figure 3 has two possible interpretations: The activity of
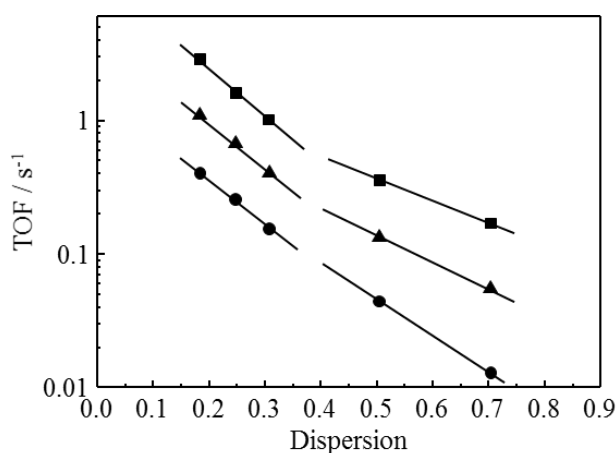


**Fig. 3** Relation between TOF and the Pt dispersion of Pt/Al$_2$O$_3$. (●) 180 °C, (▲) 200 °C and (■) 220 °C.

Pt with low dispersion was accelerated as compared to the one extrapolated from that of Pt with high dispersion, or, alternatively, the Pt with high dispersion was accelerated as compared to the Pt with low dispersion. An important point is that the value of $E_a$ increased with an increase of the Pt dispersion (Table 2). That is, in Pt with high dispersion, there was a remarkable increase the activity as the reaction temperature increased, resulting in an increase of $E_a$. Therefore, it can be found that Pt with high dispersion, i.e., small particle diameter, has the potential ability to enhance the CO oxidation activity as compared to the one with low dispersion. Also, it supposes that Pt with high dispersion is suitable for an exothermic reaction such as hydrogen combustion under mild conditions.

In conclusion, CO oxidation activity of α-Al$_2$O$_3$ supported Pt catalyst, prepared by a dry impregnation method was studied. An ignition-extinction phenomenon was observed under O$_2$ rich conditions of O$_2$/CO=10. The activation energy decreased with a decrease of Pt dispersion, i.e. an increase of Pt diameter. Further, the catalytic activity increased with a decrease of Pt dispersion, showing a structure sensitivity with negative particle effect. Two different activities were observed in the relation between TOF and the Pt dispersion: the Pt/Al$_2$O$_3$ with rather high dispersion exhibited higher TOF than the expected one extrapolated from the low dispersion catalysts. This indicates that Pt nanoparticles with small particle diameter possess a potential ability to enhance CO oxidation activity.

**References**
[1] J. Shen, N. Semagina, ACS Catal. 4 (2014) 268.
[2] B. L. Cushing, V. L. Kolesnichenko, C. J. O'Connor, Chem. Rev. 104 (2004) 3893.
[3] Y. Xia, Y. Xiong, B. Lim, S. E. Skrabalak, Angew. Chem. Int. Ed. 48 (2009) 60.
[4] M. Inoue, H. Shingen, T. Kitami, S. Akamaru, A. Taguchi, Y. Kawamoto, A. Tada, K. Ohtawa, K. Ohba, M. Matsuyama, K. Watanabe, I. Tsubone, T. Abe, J. Phys. Chem. C 112 (2008) 1479.
[5] T. Abe, M. Tanizawa, K. Watanabe, A. Taguchi, Ener. Environment. Sci. 2 (2009) 315.
[6] A. Taguchi, M. Inoue, C. Hiromi, M. Tanizawa, T. Kitami, T. Abe, Vacuum 83 (2009) 575.

[7] A. Taguchi, T. Ozaki, Annual Report of Hydrogen Isotope Research Center, Univ. Toyama 35 (2015) 13.

[8] I. H. Son, M. Shamsuzzoha, A. M. Lane, J. Catal. 210 (2002) 460.

[9] Y. -F. Han, M. J. Kahlich, M. Kinne, R. J. Behm, Appl. Catal. B: Environ. 50 (2004) 209.

[10] P. J. Berlowitz, C. H. F. Peden, D. Wayne Goodman, J. Phys. Chem. 92 (1988) 5213.

[11] A. Bourane, D. Bianchi, J. Catal. 222 (2004) 499.

[12] K. Arnby, A. Törncrona, B. Andersson, M. Skoglundh, J. Catal. 221 (2004) 252.

[13] A. Wille, E. Fridell, Appl. Catal. B: Environ. 70 (2007) 294.

[14] G. S. Zafiris, R. J. Gorte, J. Catal. 140 (1993) 418.

[15] F. J. Gracia, L. Bollmann, E. E. Wolf, J. T. Miller, A. J. Kropf, J. Catal. 220 (2003) 382.

[16] A. Bourane, D. Bianchi, J. Catal. 202 (2001) 34.

[17] R. H. Venderbosch, W. Prins, W. P. M. van Swaaij, Chem. Eng. Sci. 53 (1998) 3355.

[18] R. H. Nibbelke, M. A. J. Campman, J. H. B. Hoebink, G. B. Marin, J. Catal. 171 (1997) 358.

[19] M. Che, C. O. Bennett, Adv. Catal. 36 (1989) 55.

[20] B. Atalik, D. Uner, J. Catal. 241 (2006) 268.

[21] A. Bourane, S. Derrouiche, D. Bianchi, J. Catal. 228 (2004) 288.